Rotating Bose-Einstein condensates with a finite number of atoms confined in a ring potential: Spontaneous symmetry breaking beyond the mean-field approximation

A. Roussou,[1] J. Smyrnakis,[2] M. Magiropoulos,[2] Nikolaos K. Efremidis,[1] and G. M. Kavoulakis[2,*]

[1]*Department of Applied Mathematics, University of Crete, GR-71004 Heraklion, Greece*
[2]*Technological Education Institute of Crete, P.O. Box 1939, GR-71004 Heraklion, Greece*

Motivated by recent experiments on Bose-Einstein condensed atoms which rotate in annular and/or toroidal traps, we study the effect of the finiteness of the atom number N on the states of lowest energy for a fixed expectation value of the angular momentum, under periodic boundary conditions. To attack this problem, we develop a general strategy, considering a linear superposition of the eigenstates of the many-body Hamiltonian, with amplitudes that we extract from the mean-field approximation. This many-body state breaks the symmetry of the Hamiltonian; it has the same energy to leading order in N as the mean-field state and the corresponding eigenstate of the Hamiltonian, however, it has a lower energy to subleading order in N and thus it is energetically favorable.

I. INTRODUCTION

Several recent experiments in the field of cold atomic gases have managed to rotate, and even create, persistent currents in clouds of Bose-Einstein condensed atoms which are confined in annular and/or toroidal traps [1–8]. Furthermore, the phenomenon of hysteresis has also been observed in an annular trap [9]. Thus, a question which arises naturally from these experiments is, What is the state of lowest energy of the atoms for a fixed expectation value of their angular momentum?

Within the mean-field, Gross-Pitaevskii approximation the answer to this question is given by the well-known solitary-wave solutions [10,11], which have been investigated thoroughly [12]. When a trapping potential is present—as in the case of cold atomic gases—interesting phenomena arise. The easiest problem is that of an infinite system in the longitudinal direction, with a very tight trapping potential in the transverse direction. In this case the transverse degrees of freedom are frozen and the problem essentially reduces to that of an infinite line. As the transverse trapping potential becomes less tight and/or the interaction strength increases, the transverse degrees of freedom start to play a role, and as a result deviations from the standard quadratic nonlinear Schrödinger equation [13] arise.

Another interesting possibility is that of a ringlike trap, where one has to impose periodic boundary conditions. In this case the solutions are given by Jacobi elliptic functions [14,15]. Depending on the ratio between the coherence length and the periphery of the ring the density of these solutions is either sinusoidal or exponentially localized [15]. In an infinite system the "dark" solution (i.e., the one with a density notch) is also static. On the other hand—as a result of the periodic boundary conditions—in a ring of a finite length the dark solitary wave has a finite velocity, while the static solitary-wave solution is "gray" (i.e., the lowest value of the density is nonzero), however, no solution exists which is both dark and static [15].

The situation becomes much less clear when one wants to introduce correlations and go beyond the mean-field approximation [16,17], which is actually the subject of the present study. More specifically, in what follows, we investigate the effect of the finiteness of the atom number N (assumed to be of order unity) on the state of lowest energy, for a fixed expectation value of the angular momentum. We stress that this question not only is interesting theoretically, but also is experimentally relevant, since recent experiments have managed to trap and detect very small numbers of atoms, see, e.g., Ref. [18] and also Ref. [19]. We should also mention that other studies [20–22] have investigated a closely related question, i.e., the relationship between the "classical" and the "quantum" solitons, according to their terminology.

To go beyond the mean-field approximation the method of diagonalization of the many-body Hamiltonian may be used. The questions which are associated with the energy of the system (i.e., the dispersion relation and the velocity of propagation of the waves, which is given by the slope of the dispersion relation) are attacked in a straightforward way from the eigenvalues of the Hamiltonian. On the other hand, extracting the density is much more challenging, since the eigenstates that one gets from the diagonalization of the many-body Hamiltonian are also eigenstates of the angular momentum and thus they are rotationally invariant. Still, the physically relevant solutions are the ones which break the axial symmetry of the Hamiltonian and clearly are not eigenstates of the angular momentum.

To answer the question that we are interested in, it is instructive to recall that the energy of the mean-field state for some fixed expectation value of the angular momentum coincides to leading order in N with that of the corresponding "yrast" state [23] (an yrast state is the lowest-energy eigenstate of the Hamiltonian and is also an eigenstate of the angular momentum), however, the yrast state has a lower energy to subleading order in N.

Having this in mind, we adopt the following strategy, which is based on the minimization of the energy: First of all, we evaluate the yrast states (diagonalizing the many-body Hamiltonian). Then, we evaluate the corresponding product, mean-field-like many-body state. Projecting this state on the

*kavoulak@cs.teicrete.gr

yrast state of some given angular momentum, we evaluate the amplitude that corresponds to the yrast state of this specific value of the angular momentum. Using these amplitudes, we thus construct a many-body state which is a linear superposition of yrast states. This state has an energy which coincides to leading order in N with that of the corresponding yrast state and of the mean-field state, but it has a lower energy to subleading order in N, lower even than the yrast state, provided that the effective interaction between the atoms is repulsive.

In what follows we first describe our model in Sec. II. In Sec. III we present the strategy that we follow for the construction of the many-body state. In Sec. IV we apply our method to the case of weak interactions, where we solve the (two-state) problem analytically. In Sec. V we go beyond the two-state model, presenting our numerical results and the finite-N corrections that we are interested in. In Sec. VI we investigate the asymptotic form of the many-body state, which reduces to the well-known state of the mean-field approximation in the appropriate limit of a large atom number. In Sec. VII we discuss the experimental relevance of our study. Finally, in Sec. VIII we give a summary of the main results and our conclusions.

II. MODEL AND GENERAL CONSIDERATIONS

We assume for simplicity one-dimensional motion of bosonic atoms under periodic boundary conditions, as in a ring potential. This assumption is valid provided that the interaction energy is much lower than the quantum of energy of the trapping potential in the transverse direction, in which case the transverse degrees of freedom are frozen.

If $\hat{a}_m$ and $\hat{a}_m^\dagger$ are annihilation and creation operators of an atom with angular momentum $m\hbar$, the Hamiltonian that we consider has the form

$$\hat{H} = \frac{\hbar^2}{2MR^2} \sum_{m=m_{\min}}^{m=m_{\max}} m^2 \hat{a}_m^\dagger \hat{a}_m + \frac{U}{2} \sum_{m+n=k+l} \hat{a}_m^\dagger \hat{a}_n^\dagger a_k a_l, \quad (1)$$

where $m_{\min}$ and $m_{\max}$ are the lowest and the highest values of m that we consider, M is the atom mass, R is the radius of the ring, and U is the matrix element for elastic s-wave atom-atom collisions (assumed to be positive). There are thus two energy scales in the problem, namely, the kinetic energy per particle $\epsilon = \hbar^2/(2MR^2)$ associated with the motion of the atoms along the ring, and the interaction energy per particle, which for a homogeneous gas is equal to $(N-1)U/2$. It is thus convenient to introduce the dimensionless quantity γ as the ratio between the interaction energy $(N-1)U$ and the kinetic energy ϵ, $\gamma = (N-1)U/\epsilon$.

III. CONSTRUCTING THE MANY-BODY STATE AS A SUPERPOSITION OF YRAST STATES

The first step in our calculation is the evaluation of the yrast states $|\Phi_{\mathrm{ex}}(L)\rangle$, which are eigenstates of the Hamiltonian $\hat{H}$, of the operator of the angular momentum $\hat{L}$, and of the number operator $\hat{N}$. As mentioned above, the Hamiltonian is axially symmetric and thus the eigenstates respect this symmetry, which implies that the corresponding single-particle density distribution is axially symmetric. Indeed, if $\hat{\Psi}(\theta)$ is the

destruction operator of a particle at an angle θ, then the single-particle density is

$$\begin{aligned}
n(\theta) &= \langle \Phi_{\mathrm{ex}}(L)|\hat{\Psi}^\dagger(\theta)\hat{\Psi}(\theta)|\Phi_{\mathrm{ex}}(L)\rangle \\
&= \frac{1}{2\pi R} \sum_{m,m'} \langle \Phi_{\mathrm{ex}}(L)|\hat{a}_m^\dagger \hat{a}_{m'}|\Phi_{\mathrm{ex}}(L)\rangle \, e^{i(m'-m)\theta} \\
&= \frac{N}{2\pi R}, \quad (2)
\end{aligned}$$

i.e., $n(\theta)$ is spatially independent and equal to the mean density for any value of L, since the matrix elements appearing above are diagonal.

On the other hand, the physically relevant solutions are not axially symmetric (in general), and this is a major problem. Actually, this problem has a much more general aspect, namely, the relationship between the mean-field solutions, which break the axial symmetry of the problem, and the eigenstates of the many-body Hamiltonian—where one is working with eigenstates of the angular momentum too, and as a result, they respect the axial symmetry of the problem. Here the general strategy that we develop allows us to extract the spatially dependent single-particle density distribution from the yrast, many-body eigenstates, going beyond the mean-field approximation.

It should be mentioned that a method that is often used to overcome this difficulty of breaking of the axial symmetry is to introduce correlation functions, for example [24],

$$n^{(2)}(\theta,\theta_0) \propto \langle \Phi_{\mathrm{ex}}(L)|\hat{\Psi}^\dagger(\theta)\hat{\Psi}^\dagger(\theta_0)\hat{\Psi}(\theta_0)\hat{\Psi}(\theta)|\Phi_{\mathrm{ex}}(L)\rangle, \quad (3)$$

where θ_0 is some reference point. While this method does indeed break the axial symmetry and allows us to get a qualitative answer, it cannot be trusted quantitatively. The easiest example is that of weak interactions (examined in detail below), where it turns out that

$$\begin{aligned}
n^{(2)}(\theta,\theta_0) &\propto [N(N-1) + 2L(N-L)\cos(\theta - \theta_0)] \\
&\propto (1 - 1/N) + 2\ell(1-\ell)\cos(\theta - \theta_0), \quad (4)
\end{aligned}$$

where $\ell = L/N$. The above expression cannot in any way be related to the density that results from the mean-field approximation,

$$n_{\mathrm{MF}}(\theta) = \frac{N}{2\pi R}(1 + 2\sqrt{\ell(1-\ell)}\cos\theta), \quad (5)$$

not even in the limit of large values of N. (In the above expression we have assumed that the arbitrary position of the minimum of the density is at $\theta = 0$.) Therefore, we conclude that $n^{(2)}(\theta,\theta_0)$ cannot be used for quantitative comparisons.

The way that we proceed is thus the following. We introduce an essentially variational many-body state, namely,

$$|\Phi(\ell_0)\rangle = \mathcal{C} \sum_{L=L_{\min}}^{L_{\max}} \langle \Phi_{\mathrm{ex}}(L)|\Phi_{\mathrm{MF}}(\ell_0)\rangle \, |\Phi_{\mathrm{ex}}(L)\rangle, \quad (6)$$

where $\mathcal{C}$ is the normalization constant. In other words, we take the inner product between the mean-field state with some angular momentum per atom $\ell_0\hbar$, $|\Phi_{\mathrm{MF}}(\ell_0)\rangle$, and some yrast state with total angular momentum $L\hbar$, $|\Phi_{\mathrm{ex}}(L)\rangle$, to get the amplitudes $\langle \Phi_{\mathrm{ex}}(L)|\Phi_{\mathrm{MF}}(\ell_0)\rangle$. From these amplitudes we then construct a linear superposition of eigenstates $|\Phi_{\mathrm{ex}}(L)\rangle$, which constitute the many-body state $|\Phi(\ell_0)\rangle$.

This state has the following crucial features: (i) it has the desired expectation value of the angular momentum; (ii) to leading order in N it has the same energy as the mean-field state, as well as the yrast state, but it has a lower energy to subleading order in N; (iii) it gives the same single-particle density distribution as the mean-field state for large values of N; and (iv) it is not fragmented.

Turning to $|\Phi_{MF}(\ell_0)\rangle$, this is a product many-body state, which corresponds to the order parameter of the mean-field approximation; obviously we work in the same basis of single-particle states, with $m_{min} \leqslant m \leqslant m_{max}$, as in the method of diagonalization,

$$|\Phi_{MF}(\ell_0)\rangle = \frac{1}{\sqrt{N!}}\left(\sum_{m=m_{min}}^{m_{max}} c_m \hat{a}_m^\dagger\right)^N |0\rangle, \qquad (7)$$

where $|0\rangle$ denotes the vacuum; also, c_m are real, variational parameters, which we evaluate by minimizing the corresponding expectation value of the energy

$$E_{MF}(\ell_0) = N\frac{\hbar^2}{2MR^2}\sum_{m=m_{min}}^{m_{max}} m^2 c_m^2$$
$$+ \frac{1}{2}N(N-1)U\int\left|\sum_{m=m_{min}}^{m_{max}} c_m\phi_m\right|^4 d\theta. \quad (8)$$

Here $\phi_m = e^{im\theta}/\sqrt{2\pi}$ are the single-particle eigenstates of the ring potential with an eigenvalue of the angular momentum equal to $m\hbar$ and an eigenenergy $\epsilon_m = m^2\epsilon$. The normalization imposes the constraint $\sum c_m^2 = 1$, while there is the additional constraint that comes from the expectation value of the angular momentum being $\ell_0 = L_0/N$, $\sum m c_m^2 = \ell_0$.

IV. RESULTS OF OUR METHOD FOR WEAK INTERACTIONS

We start with the limit of weak interactions, where we can solve this problem analytically, and then proceed with the more general problem of stronger interactions. To define the limits of "weak" and "strong" interactions let us introduce quite generally the ratio between the interaction energy per particle of the homogeneous gas $(N-1)U/2$ and the kinetic energy $\epsilon_m = m^2\hbar^2/(2MR^2)$, which is $\gamma/(2m^2)$. For some given value of γ, setting $\gamma/(2m^2) \sim 1$, the maximum value of $|m|$ has to be (much) larger than $\sqrt{\gamma/2}$ in order to achieve convergence. In terms of length scales, the parameter $\sqrt{\gamma}$ gives the ratio between the radius of the ring R and the coherence length ξ (ignoring terms of order unity). The limit $\gamma \ll 1$ defines the regime of weak interactions, where $\xi \gg R$, while for $1 \ll \gamma \ll N^2$, then $R/N \ll \xi \ll R$, which is the "Thomas-Fermi" limit. When γ becomes of order N^2, then the system approaches the Tonks-Girardeau limit, where the coherence length ξ becomes comparable to the interparticle spacing R/N and correlations play a crucial role.

When $\gamma \ll 1$ one may work with the single-particle states ϕ_0 and ϕ_1 only. In this case $|\Phi_{ex}(L)\rangle$ has the very simple form (because of the two constraints)

$$|\Phi_{ex}(L)\rangle = |0^{N-L}, 1^L\rangle. \qquad (9)$$

In the above notation state ϕ_0 has $N-L$ atoms, and state ϕ_1 has L atoms.

The mean-field, many-body state is

$$|\Phi_{MF}(\ell_0)\rangle = \frac{1}{\sqrt{N!}}(c_0\hat{a}_0^\dagger + c_1\hat{a}_1^\dagger)^N|0\rangle$$
$$= \sum_{L=0}^{N}\frac{\sqrt{N!}}{(N-L)!L!}c_0^{N-L}c_1^L(\hat{a}_0^\dagger)^{N-L}(\hat{a}_1^\dagger)^L|0\rangle$$
$$= \sum_{L=0}^{N}\frac{\sqrt{N!}}{\sqrt{(N-L)!L!}}c_0^{N-L}c_1^L|0^{N-L},1^L\rangle$$
$$\equiv \sum_{L=0}^{N}d_L(\ell_0)|0^{N-L},1^L\rangle. \qquad (10)$$

The actual value of c_0^2 is $1 - \ell_0$, while $c_1^2 = \ell_0$.

The amplitudes of the above state of Eq. (10) have the interesting feature that

$$|d_L(\ell_0)|^2 \equiv \frac{N!}{(N-L)!L!}c_0^{2(N-L)}c_1^{2L}$$
$$\approx \frac{e^{-(L-N\ell_0)^2/[2N\ell_0(1-\ell_0)]}}{\sqrt{2\pi N\ell_0(1-\ell_0)}}\left[1 + O\left(\frac{1}{\sqrt{N}}\right)\right], \quad (11)$$

where the approximate expression holds for large N and $\ell_0(1-\ell_0)$ not close to 0. Therefore, $|d_L|^2$ is a Gaussian, with its peak at $L_0 = N\ell_0$ (scaling as N) and a width which is of order $\sqrt{N}$, which becomes a delta function in the limit of large N. The above observations are generic features and not specific to the two-state model and thus are central in the analysis that follows.

In the final step of our calculation we evaluate $|\Phi(\ell_0)\rangle$, which is, as described earlier,

$$|\Phi(\ell_0)\rangle = \mathcal{C}\sum_{L=0}^{N}d_L(\ell_0)|0^{N-L},1^L\rangle. \qquad (12)$$

In the two-state approximation, $|\Phi(\ell_0)\rangle$ coincides with $|\Phi_{MF}(\ell_0)\rangle$. However, we stress that this is not a general result, as we explain below.

The single-particle density matrix of $|\Phi(\ell_0)\rangle$, $\rho_{ij} = \langle\Phi(\ell_0)|a_i^\dagger a_j|\Phi(\ell_0)\rangle$ (with $i,j = 0,1$), is

$$\rho = N\begin{pmatrix} c_0^2 & c_0c_1 \\ c_0c_1 & c_1^2 \end{pmatrix}.$$

The two eigenvalues are $\lambda = 0$ and $\lambda = 1$ (the determinant of the above matrix vanishes and thus one of the eigenvalues has to vanish). The state $|\Phi(\ell_0)\rangle$ is not fragmented, as one expects. The eigenvector that corresponds to $\lambda = 1$ is the expected one, namely, $\psi = c_0\phi_0 + c_1\phi_1$. The single-particle density distribution in $|\Phi(\ell_0)\rangle$ is given by

$$n(\theta) = \langle\Phi(\ell_0)|\hat{\Psi}^\dagger(\theta)\hat{\Psi}(\theta)|\Phi(\ell_0)\rangle$$
$$= \frac{N}{2\pi R}[1 + 2|c_0||c_1|\cos(\theta - \theta_0)]$$
$$= \frac{N}{2\pi R}[1 + 2\sqrt{\ell_0(1-\ell_0)}\cos(\theta - \theta_0)], \quad (13)$$

where θ_0 is the relative phase between c_0 and c_1. This phase is arbitrary, reflecting the rotational invariance of the

Hamiltonian; assuming that c_0 and c_1 are real, it is equal to either 0 or π. However, this degeneracy is lifted when the symmetry is broken (see more in the following paragraph). The result of Eq. (13) coincides with that of Eq. (5), and therefore in the two-state model the density that one gets from our many-body state $|\Phi(\ell_0)\rangle$ is the same as the one derived from the Jacobi (sinusoidal) solutions of the mean-field Gross-Pitaevskii approximation.

Furthermore, the expectation value of the energy $\mathcal{E}$ in the state $|\Phi(\ell_0)\rangle$ is

$$\mathcal{E} - \frac{U}{2}N(N-1) = \frac{\hbar^2 L_0}{2MR^2} + UL_0(N-L_0)(1 - 1/N), \tag{14}$$

where again the phase θ_0 does not appear in the energy due to the assumed axial symmetry of the Hamiltonian. When a weak symmetry-breaking potential $\Delta V = V_0 \cos\theta$ is added to the Hamiltonian, then

$$\mathcal{E} - UN(N-1)/2 = \frac{\hbar^2 L_0}{2MR^2} + UL_0(N-L_0)(1 - 1/N)$$
$$+ \cos\theta_0 N V_0 \sqrt{\ell_0(1-\ell_0)}/2. \tag{15}$$

Here we see an explicit dependence of the energy on θ_0. Obviously θ_0 has to take the value π in order for the energy to be minimized. As a result, the single-particle density is $n(\theta) = N(1 - 2\sqrt{\ell(1-\ell)}\cos\theta)/(2\pi R)$, and thus the minimum of the density is at $\theta = 0$, where the value of the potential is maximum.

In Eqs. (14) and (15) above we observe that to leading order in N the interaction energy agrees with that of the eigenstates $|0^{N-L_0}, 1^{L_0}\rangle$, $\mathcal{E}_{\mathrm{ex}}$, which is

$$\mathcal{E}_{\mathrm{ex}} - \frac{U}{2}N(N-1) = \frac{\hbar^2 L_0}{2MR^2} + UL_0(N-L_0), \tag{16}$$

but is lower to subleading order. This result is due to the fact that the dispersion relation has a negative curvature and the fact that $|\Phi(\ell_0)\rangle$ samples other states—of order $\sqrt{N}$–around the "pure" state $|\Phi_{\mathrm{ex}}(L_0)\rangle = |0^{N-L_0}, 1^{L_0}\rangle$. Actually, this lowering of the energy to subleading order in N of the state that breaks the axial symmetry reflects precisely this fact, namely that the curvature of the dispersion relation is negative (provided that the effective interaction is repulsive).

Indeed, quite generally, a distribution $P(L) \propto e^{-(L-L_0)^2/N}/\sqrt{N}$ [see Eq. (12)] gives an average of $UL(N-L)$ that differs from $UL_0(N-L_0)$ [see Eq. (16)], which is proportional to $-UN$, as in Eq. (14),

$$U\langle L(N-L)\rangle - UL_0(N-L_0) \propto -UN\,\mathrm{erf}(L_0/\sqrt{N})$$
$$\approx -UN, \tag{17}$$

where $\mathrm{erf}(x)$ is the error function.

V. BEYOND THE TWO-STATE MODEL: FINITE-*N* CORRECTIONS AND NUMERICAL RESULTS

The two-state model discussed above has the advantage that all the calculations may be performed analytically. In addition, it provides an accurate description of $|\Phi(\ell_0)\rangle$ in the limit of weak interactions, $\gamma \ll 1$. The results of the previous section

demonstrate that in this limit the state $|\Phi(\ell_0)\rangle$—even in a system with a finite number of atoms N—essentially coincides with one of the mean-field approximation (which, in the limit of weak interactions, gives a sinusoidal density distribution).

On the other hand, as we also saw earlier, the very drastic restriction to the states ϕ_0 and ϕ_1 (only) forces the yrast states to have the trivial form $|0^{N-L}, 1^L\rangle$ and therefore all the angular momentum is carried by the single-particle state ϕ_1. It is thus necessary to work in a more extended space. In the interval $0 \leqslant \ell \leqslant 1$ and for relatively stronger interactions in addition to ϕ_0 and ϕ_1, ϕ_2 and ϕ_{-1} have the most significant contribution, while if one wants to go even further ϕ_3 and ϕ_{-2} have to be included too, and so on, as Bloch's theorem implies [25].

Before we turn to a higher truncation, it is instructive to examine the case with ϕ_0, ϕ_1, and ϕ_2, only. In this subspace the yrast states have the form

$$|\Phi_{\mathrm{ex}}(L)\rangle = \sum_m (-1)^m b_m |0^{N-L+m}, 1^{L-2m}, 2^m\rangle, \tag{18}$$

where the amplitudes b_m are Gaussian distributed [23]. The corresponding mean-field, product many-body state has the form

$$|\Phi_{\mathrm{MF}}(\ell_0)\rangle = \frac{1}{\sqrt{N!}}(c_0 \hat{a}_0^\dagger + c_1 \hat{a}_1^\dagger + c_2 \hat{a}_2^\dagger)^N |0\rangle$$
$$= \sum_{k=0}^N \sum_{m=0}^k \frac{\sqrt{N!}\, c_0^{N-k} c_1^{k-m} c_2^m}{\sqrt{(N-k)!(k-m)!m!}} |0^{N-k}, 1^{k-m}, 2^m\rangle$$
$$\equiv \sum_{k=0}^N \sum_{m=0}^k d_{m,k} |0^{N-k}, 1^{k-m}, 2^m\rangle. \tag{19}$$

Taking the inner product between state $|\Phi_{\mathrm{ex}}(L)\rangle$ and state $|\Phi_{\mathrm{MF}}(\ell_0)\rangle$ forces the index k to be equal to $L - m$ and therefore the only nonzero amplitudes are $d_{m,L-m}$, which are also Gaussian distributed. When more single-particle states are included in the calculation the general picture is the same, with the only difference being that one has a multidimensional space; if r is the number of single-particle states, the dimensionality is $r - 2$, because of the two constraints. In each direction in this space one still obtains Gaussian distributions and on a qualitative level the final result is essentially the same.

We proceed now with the calculation within states ϕ_{-2}, ϕ_{-1}, ϕ_0, ϕ_1, ϕ_2, and ϕ_3. We stress that γ has to be sufficiently large in order to have a significant occupancy of the states other than the ones with $m = 0$ and $m = 1$, since otherwise one goes back to the two-state model described earlier. In addition, we have to make sure that we have reached convergence with respect to the number of single-particle states that are considered and, finally, we have to ensure that Bloch's theorem [25] is not violated. As also described above, we first evaluate the yrast states $|\Phi_{\mathrm{ex}}(L)\rangle$ for $-2N \leqslant L \leqslant 3N$, diagonalizing the many-body Hamiltonian. We also evaluate $|\Phi_{\mathrm{MF}}(\ell_0)\rangle$

$$|\Phi_{\mathrm{MF}}(\ell_0)\rangle = \frac{1}{\sqrt{N!}}\left(\sum_{m=-2}^{m=3} c_m \hat{a}_m^\dagger\right)^N |0\rangle, \tag{20}$$

where c_{-2}, c_{-1}, c_0, c_1, c_2, and c_3 are evaluated from the constraint minimization of the energy. In the final step we
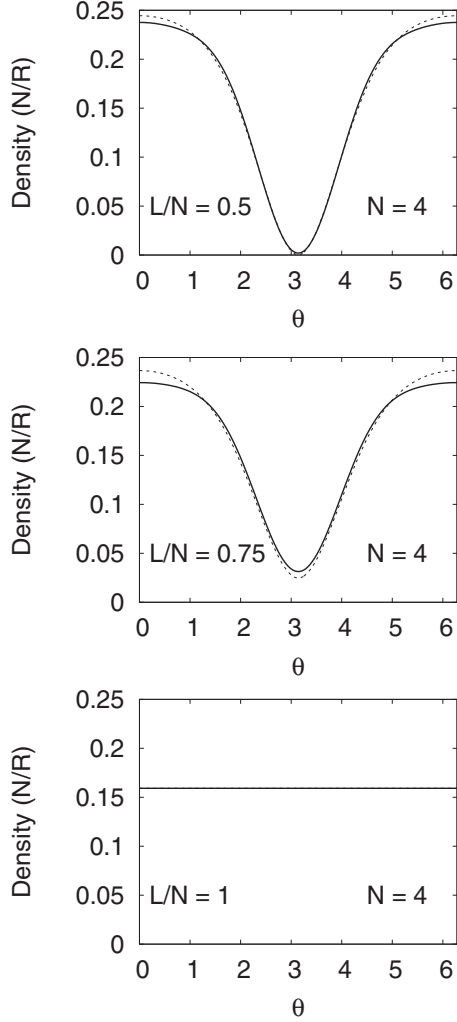
FIG. 1. Solid lines: The single-particle density distribution $n(\theta)$ corresponding to $|\Phi(\ell)\rangle$ of a finite system of atoms, within the space of states with $m = -2, \ldots, 3$, for $N = 4$ atoms, $\gamma = (N-1)U/\epsilon = 0.9$, and $\ell = L/N = 0.50, 0.75$, and 1.00, from top to bottom. Dashed lines: The single-particle density distribution $n_{MF}(\theta)$ corresponding to $|\Phi_{MF}(\ell)\rangle$, derived within the mean-field approximation, via the minimization of the energy, for the same set of parameters.

evaluate $|\Phi(\ell_0)\rangle$ using Eq. (6), which then gives us the single-particle density distribution (or any other observable).

In Figs. 1 and 2 we plot the corrections of the density in a finite system of atoms for various values of the angular momentum. The solid curves show the single-particle density $n(\theta)$ that corresponds to $|\Phi(\ell_0)\rangle$, while the dashed ones show the density $n_{MF}(\theta)$ that corresponds to the mean-field state $|\Phi_{MF}(\ell_0)\rangle$. In Fig. 1 $N = 4$, and in Fig. 2 $N = 8$, while $\gamma = 0.9$ in both figures. Also, ℓ_0 takes the three values $\ell_0 = 0.5, 0.75$, and 1. According to Bloch's theorem [25] for any $0 \leqslant \ell_0 \leqslant 1$, the density distribution is the same also for $\ell'_0 = 1 - \ell_0$, as well as for $\ell'_0 = \ell_0 + \kappa$, where κ is an integer. In other words, the three graphs for $\ell_0 = 1 (L = 4)$, $\ell_0 = 3/4 (L = 3)$, and $\ell_0 = 1/2 (L = 2)$ shown in Fig. 1 cover all the possible values of the angular momentum of the whole spectrum (for $N = 4$).

For $\ell_0 = 1$ both $n_{MF}(\theta)$ and $n(\theta)$ are constant, even for small values of N. We stress, however, that the two states
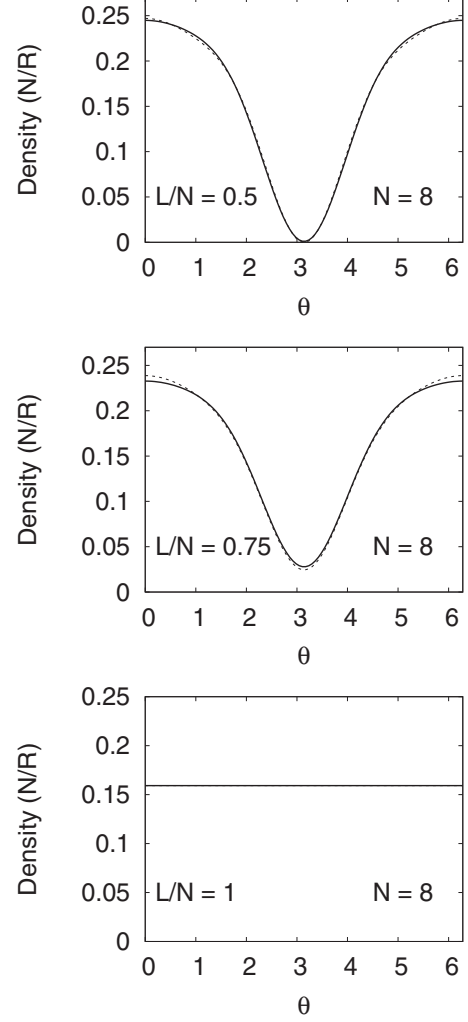

FIG. 2. Same as Fig. 1, with $N = 8$ and $\gamma = 0.9$. The difference between the two curves is hardly visible.

are different, since $|\Phi(\ell_0)\rangle$ coincides with the yrast state for $L = N = 4$. For example, even within the space with $m = 0$, 1, and 2,

$$|\Phi_{MF}(\ell_0 = 1)\rangle = |0^0, 1^4, 2^0\rangle, \qquad (21)$$

while

$$\begin{aligned}|\Phi(\ell_0 = 1)\rangle &= A_1|0^0, 1^4, 2^0\rangle + A_2|0^1, 1^2, 2^1\rangle \\ &\quad + A_3|0^2, 1^0, 2^2\rangle,\end{aligned}$$

$$(22)$$

where A_i are constants. As a result, the energy of the two states is also different (see Fig. 3, which shows the dispersion relation, which we discuss in the next section).

Returning to the density shown in Figs. 1 and 2, while for $\ell_0 = 1$ the situation is not interesting (at least with regard to the density), for $\ell_0 = 1/2$ and $\ell_0 = 3/4$ there are deviations (between the dashed and the solid curves). For $\ell_0 = 1/2$ within the mean-field approximation, the "dark" solitary wave forms and $n_{MF}(\theta)$ has a node. As shown in Fig. 1, $n(\theta)$ still has a node. The most significant deviations appear at the maxima of the density. Our state of lower energy flattens out within
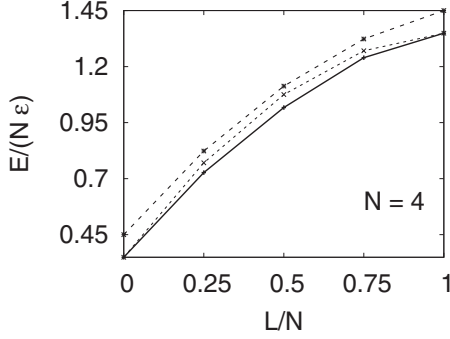
FIG. 3. The energy per particle as a function of the angular momentum per particle for $N = 4$ atoms, $\gamma = (N-1)U/\epsilon = 0.9$, and $\ell = L/N = 0.50$, 0.75, and 1.00, within the space of states with $m = -2, \ldots, 3$. The lowest curve corresponds to the expectation value of the energy of $|\Phi(\ell)\rangle$; the middle curve, to the eigenvalues of the yrast states $|\Phi_{\mathrm{ex}}(L)\rangle$; and the top curve, to the energy of the mean-field state $|\Phi_{\mathrm{MF}}(\ell)\rangle$. We stress that in the middle curve L on the x axis is the eigenvalue of $\hat{L}$, while in the other two curves L is the expectation value of $\hat{L}$.

a larger interval compared to the mean-field density. These deviations (almost) disappear for $N = 8$, as shown in Fig. 2, where γ is still 0.9 (we discuss the asymptotic behavior of $|\Phi(\ell)\rangle$ in the following section). Finally, for $\ell_0 = 3/4$, there is still a significant deviation between $n(\theta)$ and $n_{\mathrm{MF}}(\theta)$, with roughly the same characteristics as in the case $\ell_0 = 1/2$.

Although the difference between the densities is small (due to the relatively small value of γ, which makes $|c_0|$ and $|c_1|$ much larger than all the other coefficients; for example, for $\ell = 1/2$, $|c_0| = |c_1|$ is roughly seven times larger than $|c_{-1}| = |c_2|$), these results are still generic. Increasing γ will cause more pronounced differences, however, the problem becomes more demanding computationally, since we also need to make sure that convergence with respect to the single-particle states that we have considered has been achieved.

VI. ASYMPTOTIC LIMIT OF THE MANY-BODY STATE

It is crucial to confirm that the observables from the state that we have introduced coincide with those of the mean-field state in the appropriate limit of large N. The relevant limit is the one where N increases, with the ratio between the interaction energy and the kinetic energy kept fixed (which in our notation is γ).

As shown in the previous section, the density indeed approaches that of the mean-field state. Turning to the energy, as argued in Sec. IV, in the above limit, the dominant amplitude in $|\Phi(\ell_0)\rangle$ is the one that corresponds to $L_0 = N\ell_0$, which is the yrast state $|\Phi_{\mathrm{ex}}(L_0)\rangle$ with this value of $L = L_0$. As shown in Ref. [23] $|\Phi_{\mathrm{ex}}(L_0)\rangle$ has the same energy to leading order in N as the mean-field state $|\Phi_{\mathrm{MF}}(\ell_0)\rangle$, and the same result is true for $|\Phi(\ell_0)\rangle$. Therefore, all three of these states have the same energy to leading order in N.

Still, we stress that there is a clear hierarchy of the energies of the three states to subleading order in N: $|\Phi_{\mathrm{MF}}(\ell_0)\rangle$ has the highest energy, $|\Phi_{\mathrm{ex}}(L_0)\rangle$ has a lower energy, and $|\Phi(\ell_0)\rangle$ has the lowest. The first inequality has been analyzed in Ref. [23],

while the second is due to the simple reason stated earlier [see Eq. (17)].

In Fig. 3 we plot the dispersion relation, which is evaluated within the mean-field approximation, the energy of the corresponding eigenstates of the many-body Hamiltonian, and the energy of $|\Phi(\ell_0)\rangle$ that we have evaluated. In the middle curve L on the x axis is the eigenvalue of $\hat{L}$, while in the other two curves L is the expectation value of $\hat{L}$. These results provide full support of the arguments we made about the hierarchy of the energies. We should also mention that according to Bloch's theorem [25], the energy spectrum for higher values of ℓ is the one shown in Fig. 3, on top of a parabolic curve.

Turning to the question of fragmentation, the single-particle density matrix of $|\Phi(\ell_0)\rangle$, $\rho_{ij} = \langle\Phi(\ell_0)|\hat{a}_i^\dagger \hat{a}_j|\Phi(\ell_0)\rangle = c_i c_j$. This result generalizes the one we found earlier for the case of two modes only. This matrix has one eigenvalue which is equal to unity, while all the other eigenvalues vanish and indeed $|\Phi(\ell_0)\rangle$ is not fragmented. The eigenvector that corresponds to the nonzero eigenvalue is the expected one, i.e., $\sum c_m \phi_m$.

VII. EXPERIMENTAL RELEVANCE

In order to make contact with experiment, the first question is the extent to which, under typical conditions, the motion of the atoms is quasi-one-dimensional, as we have assumed here. If we consider the experiment in Ref. [9] as an example, the system is far from this limit. In that experiment, where $N \approx 4 \times 10^5$ ^{23}Na atoms were used, their chemical potential, $\mu/\hbar \approx 2\pi \times 1.7$ kHz, was much higher than the frequencies of the (annularlike) trapping potential, $\omega_1 \approx 472$ Hz and $\omega_2 \approx 188$ Hz. The dimensionless quantity that describes the transition to the one-dimensional limit may also be expressed in terms of Na/R, which has to be $\ll 1$ in this limit. Here $R \approx 19.5 \mu$m is the mean radius of the torus and/or annulus and $a \approx 28$ Å is the s-wave scattering length for atom-atom collisions. Since Na/r is $\approx 5 \times 10^2$, the system is not in the limit of quasi-one-dimensional motion.

In addition, the dimensionless parameter $\gamma = 2NaR/S$, where S is the cross section of the torus and/or annulus, for the parameters of this experiment is of the order of 1500 [26]. As a result, this experiment is performed in the Thomas-Fermi regime (see Sec. IV), where $1 \ll \gamma \ll N^2$, and the solitary waves will resemble the well-known ones of an infinite system.

According to the results of our study three conditions have to be satisfied in order for the corrections that we have predicted to be substantial. First, N should not exceed ~ 10, since otherwise the corrections will be suppressed. Also, the interaction energy has to be sufficiently strong, i.e., γ should be at least of order unity, since otherwise the system is in the limit of weak interactions, where the deviations we have found are also suppressed. Finally, Na/R has to be $\ll 1$.

If one simply reduces N under the conditions of the experiment in Ref. [9], by, e.g., a factor of order 10^5, so that N becomes equal to 4, then $Na/R \sim 5 \times 10^{-3}$, i.e., indeed it will be $\ll 1$, however $\gamma \sim 1.5 \times 10^{-2}$, i.e., γ will also become $\ll 1$, which will bring the system to the limit of weak interactions. Therefore, in addition to reducing N by a large factor, one should also decrease $S \propto 1/\sqrt{\omega_1 \omega_2}$ (by, e.g., increasing the trapping frequencies in the transverse direction), in order to make $\gamma \sim 1$.

VIII. SUMMARY AND CONCLUSIONS

To summarize, the general problem that we have investigated is the relationship between the mean-field approximation and the method of diagonalization of the many-body Hamiltonian, in connection with the spontaneous breaking of the symmetry of the Hamiltonian (assumed to be axially symmetric). While the mean-field states break the symmetry of the Hamiltonian by construction, the eigenstates of the Hamiltonian respect this symmetry, thus giving rise to a single-particle density distribution which is always axially symmetric. Still, in a real system the axial symmetry is broken, even under very weak symmetry-breaking mechanisms (if one is interested in the solutions which do not break the symmetry, these are the eigenstates of the Hamiltonian).

One of the main goals of the present study is to investigate how one breaks the symmetry, going also beyond the mean-field approximation. To achieve this goal, we make use of the mean-field approximation and then construct a linear superposition of the eigenstates of the many-body Hamiltonian. This state breaks the symmetry and is not a product state, i.e., it goes beyond the mean-field approximation. We stress that the method that we have developed is general and may be applied to other problems as well.

Another main result of our study is the actual problem where we have applied this method, namely, the finite-N corrections of the well-known solitary-wave solutions which result within the (one-dimensional) nonlinear Schrödinger equation in a finite ring. Interestingly, the state that we have used is one of "minimum uncertainty", and in a sense it is the mostly "classical". According to our results, for low interaction strengths, where the two-state model is a good approximation, the finite-N corrections are negligible and one gets back to the ordinary Jacobi solutions of the nonlinear Schrödinger equation (which are sinusoidal in this limit). For higher interaction strengths and/or small atom numbers, where more than two single-particle states need to be considered, these corrections become non-negligible and there are significant deviations between our many-body state and the mean-field state.

While we have not proven that the many-body state that we have constructed provides the absolute minimum of the energy, what we do know is that it has the same energy to leading order in N, and a lower energy to subleading order in N, compared to the mean-field state and the corresponding eigenstate of the Hamiltonian. In other words, this many-body state provides a lower bound of the energy. One subtle point in these arguments is of course that in this comparison the yrast state is an eigenstate of the operator of the angular momentum $\hat{L}$, and thus L is the corresponding eigenvalue. In the other two states, since they break the symmetry, L is the expectation value of $\hat{L}$.

When the angular momentum is an integer multiple of $\hbar$ within the mean-field approximation the density of the cloud is predicted to be homogeneous. According to our results, the single-particle density distribution remains homogeneous even for a small atom number. When the angular momentum per particle is equal to a half-integer within the mean-field approximation the "dark" solitary wave forms, which has a node in its density. According to our analysis in a system with a small atom number the single-particle density distribution still has a node, with the main effect of the finiteness appearing at the "edges" of the wave. Interestingly, a "universal" feature of the dark solitary wave is its velocity of propagation, which turns out to be $\hbar/(2MR)$ (for any interaction strength or any atom number N), as we have found numerically, essentially due to Bloch's theorem [25]. Last but not least, deviations in the density between the two states are also present in the intermediate values of the angular momentum (between 0.5 and 1). These corrections vanish in the appropriate limit of large N.

Our suggested many-body state is not a "solitary-wave state" in the strict sense of a traveling-wave solution and for this reason we have not used this terminology here. The dynamics of this many-body wave function is a problem that we are currently working on and will be analyzed in a future study.

The interaction strengths that we have considered keep us away from the correlated, Tonks-Girardeau limit. It would be interesting to try to push this calculation to this regime [21,27]. In the spirit of density functional theory, one may develop a mean-field description [28] and then use the present approach, which may still provide an accurate description of the system. We plan to get some quantitative answers on this problem in the near future.

[1] S. Gupta, K. W. Murch, K. L. Moore, T. P. Purdy, and D. M. Stamper-Kurn, Phys. Rev. Lett. **95**, 143201 (2005).

[2] S. E. Olson, M. L. Terraciano, M. Bashkansky, and F. K. Fatemi, Phys. Rev. A **76**, 061404(R) (2007).

[3] C. Ryu, M. F. Andersen, P. Cladé, V. Natarajan, K. Helmerson, and W. D. Phillips, Phys. Rev. Lett. **99**, 260401 (2007).

[4] B. E. Sherlock, M. Gildemeister, E. Owen, E. Nugent, and C. J. Foot, Phys. Rev. A **83**, 043408 (2011).

[5] A. Ramanathan, K. C. Wright, S. R. Muniz, M. Zelan, W. T. Hill, C. J. Lobb, K. Helmerson, W. D. Phillips, and G. K. Campbell, Phys. Rev. Lett. **106**, 130401 (2011).

[6] S. Moulder, S. Beattie, R. P. Smith, N. Tammuz, and Z. Hadzibabic, Phys. Rev. A **86**, 013629 (2012).

[7] C. Ryu, K. C. Henderson, and M. G. Boshier, New J. Phys. **16**, 013046 (2014).

[8] S. Beattie, S. Moulder, R. J. Fletcher, and Z. Hadzibabic, Phys. Rev. Lett. **110**, 025301 (2013).

[9] S. Eckel, J. G. Lee, F. Jendrzejewski, N. Murray, C. W. Clark, C. J. Lobb, W. D. Phillips, M. Edwards, and G. K. Campbell, Nature (London) **506**, 200 (2014).

[10] A. D. Jackson, J. Smyrnakis, M. Magiropoulos, and G. M. Kavoulakis, Europhys. Lett. **95**, 30002 (2011).

[11] R. Kanamoto, L. D. Carr, and M. Ueda, Phys. Rev. A **81**, 023625 (2010).

[12] A. C. Scott, F. Y. F. Chu, and D. W. McLaughlin, Proc. IEEE **61**, 1443 (1973); R. Rajaraman, *Solitons and Instantons* (North-Holland, Amsterdam, 1987); V. E. Zakharov and A. B. Shabat, Zh. Eksp. Teor. Fiz. **64**, 1627 (1973) [Sov. Phys. JETP **37**, 823 (1973)].

[13] A. D. Jackson, G. M. Kavoulakis, and C. J. Pethick, Phys. Rev. A **58**, 2417 (1998).

[14] L. D. Carr, C. W. Clark, and W. P. Reinhardt, Phys. Rev. A **62**, 063610 (2000).

[15] J. Smyrnakis, M. Magiropoulos, G. M. Kavoulakis, and A. D. Jackson, Phys. Rev. A **82**, 023604 (2010).

[16] C. Yannouleas and U. Landman, Rep. Prog. Phys. **70**, 2067 (2007).

[17] C. Yannouleas and U. Landman, Phys. Rev. B **84**, 165327 (2011).

[18] A. N. Wenz, G. Zürn, S. Murmann, I. Brouzos, T. Lompe, and S. Jochim, Science **342**, 457 (2013).

[19] U. Marzolino and D. Braun, Phys. Rev. A **88**, 063609 (2013).

[20] M. Wadati and M. Sakagami, J. Phys. Soc. Jpn. **53**, 1933 (1984); M. Wadati, A. Kuniba, and T. Konishi, *ibid.* **54**, 1710 (1985); J. Dziarmaga, Z. P. Karkuszewski, and K. Sacha, Phys. Rev. A

66, 043615 (2002); D. Delande and K. Sacha, Phys. Rev. Lett. **112**, 040402 (2014); A. Syrwid and K. Sacha, Phys. Rev. A **92**, 032110 (2015); A. Syrwid, M. Brewczyk, M. Gajda, and K. Sacha, *ibid.* **94**, 023623 (2016).

[21] M. D. Girardeau and E. M. Wright, Phys. Rev. Lett. **84**, 5691 (2000).

[22] J. Sato, R. Kanamoto, E. Kaminishi, and T. Deguchi, Phys. Rev. Lett. **108**, 110401 (2012); New J. Phys. **18**, 075008 (2016).

[23] A. D. Jackson, G. M. Kavoulakis, B. Mottelson, and S. M. Reimann, Phys. Rev. Lett. **86**, 945 (2001); J. C. Cremon, A. D. Jackson, E. Ö. Karabulut, G. M. Kavoulakis, B. R. Mottelson, and S. M. Reimann, Phys. Rev. A **91**, 033623 (2015).

[24] H. Saarikoski, S. M. Reimann, A. Harju, and M. Manninen, Rev. Mod. Phys. **82**, 2785 (2010).

[25] F. Bloch, Phys. Rev. A **7**, 2187 (1973).

[26] A. Roussou, G. D. Tsibidis, J. Smyrnakis, M. Magiropoulos, Nikolaos K. Efremidis, A. D. Jackson, and G. M. Kavoulakis, Phys. Rev. A **91**, 023613 (2015).

[27] I. Romanovsky, C. Yannouleas, L. O. Baksmaty, and U. Landman, Phys. Rev. Lett. **97**, 090401 (2006).

[28] E. B. Kolomeisky, T. J. Newman, J. P. Straley, and X. Qi, Phys. Rev. Lett. **85**, 1146 (2000).